Nonlinear Dyn (2024) 112:681–692
https://doi.org/10.1007/s11071-023-09061-x

ORIGINAL PAPER

Coexisting multi-period and chaotic attractor in fully connected system via adaptive multi-body interaction control

Qinrui Dai

Received: 2 April 2023 / Accepted: 9 September 2023 / Published online: 21 November 2023

Abstract Multi-body interaction has been proved to exist widely in the real world. To verify the influence of multi-body interactive feedback on the dynamics of system, a novel adaptive time-delay multi-body interaction control is proposed in this work. The global stability and local bifurcation of the controlled system are investigated. Applying the controller to ternary and quaternary neural network models, we find that there are complex dynamical phenomena in the controlled networks. When the time delay is small, only a single asymptotically stable solution is observed. With the increase in the time delay, the system undergoes a periodic solution induced by Hopf bifurcation. However, with further increase in the time delay, multi-periodic solutions and multiple chaotic attractors coexist near the equilibrium point. Compared with the traditional controller, the adaptive multi-body feedback controller can make the neural network system without non-trivial phenomenon enable complex coexistence phenomenon, only by controlling one neuron node.

Keywords Multi-body feedback · Adaptive control · Bifurcation · Chaos

Q. Dai (✉)
School of Mathematics and Statistics, Wuhan University, Wuhan 430072, China
e-mail: daiqinrui@whu.edu.cn

1 Introduction

As a branch of modern mathematics, dynamical system is to study the change of system properties over time. Bifurcation and chaos are important tools for describing the dynamics and topological structure of differential equation systems, mainly involving single-parameter codimension-one bifurcation and multi-parameter codimension-two bifurcation [1–4], as well as chaotic attractors [5–7]. There are many routes to chaos from the equilibrium point, such as period-doubling [8], torus bifurcation [9], homoclinic manifold entanglement [10], etc.

Multistability, coexistence of multiple periods and chaotic attractors play crucial roles in the dynamics of nonlinear systems, and the specific mechanism can be investigated from the perspective of bifurcation and control. Nowadays, a great number of effective controllers have been proposed to improve the performance and dynamics of the system, including adaptive control [11], sliding mode control [12], intermittent control [13], etc. In addition, some scholars focus on the bifurcation properties of controlled systems, thus forming a unique perspective of bifurcation control [14, 15], in which hopf bifurcation is widely concerned because it is a dynamic process from point to period in phase space [16, 17]. However, these controllers are only limited to self-feedback or two-body interaction, which is of course suitable for low-order two-dimensional systems, but applying them to high-dimensional nonlinear systems does not significantly improve the dynamics. Recently, some research results show that multi-body interaction widely exists in the real world, such as brain neural network [18], nematode network [19], etc. Therefore, the feedback effect generated by multi-body interaction should not be ignored when we conduct high-dimensional system modeling. Furthermore, due to the limitation of speed, there is usually time-delay [20,21] in information transmission between different individuals. Accordingly, in the design of some feedback controllers, time-delay is typically considered and used as a key parameter to analyze the dynamics of system.

Motivated by the above discussion and analysis, this paper investigates the stability and bifurcation behavior of a fully connected system via adaptive multi-body interaction control. The main innovation and contribution of this paper can be listed as follows.

1. Considering the multi-body effect of information transmission, we propose an adaptive delayed multi-body interaction control for fully connected system.
2. We analyze the local and global stability of the controlled system, and with time delay as the key parameter, the existence condition and critical value of Hopf bifurcation are obtained.
3. Applying the controller to two fully connected delayed neural network models, it is found that the controlled network has the coexistence of multi-periodic and multi-chaotic attractors which has never existed before.

The rest of the paper is arranged as follows. In the Sect. 2, we design an adaptive multi-body interactive feedback controller for a fully connected system with time delay. The existence of Hopf bifurcation is proved, and the conditions of global stability for the controlled system are given. In Sect. 3, the controller is applied to two specific neural network models to investigate its impact on the network dynamics. We find that the controlled network undergoes complex coexistence phenomena near the equilibrium point, especially the coexistence of multi-period and multi-chaotic attractors. Section 4 gives a brief summary and prospects for our future work.

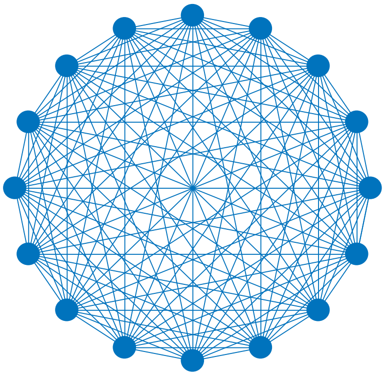

Fig. 1 Schematic diagram of a fully connected system with 16 nodes

2 Design of controller and dynamic analysis of system

In this section, we design a multi-body interaction controller for fully connected system, and analyze the stability and Hopf bifurcation of the controlled system.

Definition 1 A system is called a fully connected system when each individual in the system has information exchange with the remaining individuals. (See Fig. 1).

Definition 2 The codimension of a bifurcation is the number of parameters which must be varied for the bifurcation to occur. This corresponds to the codimension of the parameter set for which the bifurcation occurs within the full space of parameters.

Consider a nonlinear functional differential equation with fully connected multiple bodies as

$$\dot{X}(t) = -\alpha X(t) + F\left(X(t-\sigma)\right), \tag{1}$$

where $X = [x_1, x_2, \cdots x_n]^T \in R^n$, $F = [f_1, f_2, \cdots, f_n]^T$ and f_i $(i = 1, 2, \cdots, n)$ are differentiable nonlinear functions. σ represents system delay.

Remark 1 Eq. (1) is a general functional differential equation with n variables, where $-\alpha X(t)$ and $F\left(X(t-\sigma)\right)$ are the linear and nonlinear parts of the system respectively, which is actually expressed in the following expansion form,

$$\begin{cases} \dot{x}_1(t) = -\alpha x_1(t) + f_1(x_1(t-\sigma), \cdots, x_n(t-\sigma)), \\ \dot{x}_2(t) = -\alpha x_2(t) + f_2(x_1(t-\sigma), \cdots, x_n(t-\sigma)), \\ \vdots \\ \dot{x}_n(t) = -\alpha x_n(t) + f_n(x_1(t-\sigma), \cdots, x_n(t-\sigma)). \end{cases}$$

At present, the research on the dynamic properties of Eq. (1) has been investigated from Hopf bifurcation to codimension-two Bautin and Hopf-Hopf bifurcations.

To guarantee the feasibility of theoretical analysis, the following assumptions are made.

Assumption 1 The nonlinear function of the system has the same expression, namely,

$$f_1(x_1, x_2, \cdots, x_n) = \cdots = f_n(x_1, x_2, \cdots, x_n) \\ = f(x_1, x_2, \cdots, x_n).$$

Assumption 2 The nonlinear function is independent with respect to all variables, that is, there are constants w_{ij} and the unary nonlinear function $g_j(x_j)$ such that $f_i(x_1, \cdots, x_n) = \sum\limits_{j=1}^{n} w_{ij} g_j(x_j)$ for $i, j = 1, 2, \cdots, n$.

Assumption 3 The unary function $g_j(x_j)$ is bounded, that is, there is a positive number l, so that $\left|g_j(x_j)\right| < l$ for $j = 1, 2, \cdots, n$.

2.1 Design of controller

The goal is to design a controller to improve the dynamic properties of system (1). The most classical self-feedback controller [22–24] is $u(t) = x(t) - x(t-\tau)$, but it only considers the delayed feedback effect of variable x on itself. Then, in light of the interaction between different individuals, the two-body controller $u(t) = y(t) - x(t-\tau)$ is applied to various nonlinear systems to achieve synchronization or topology identification [25]. When the number of interaction individuals in the system rises to three or more, the three-body interaction has to be included to describe the impact of groups on the system dynamics. For example, multi-body interaction in cooperative networks will generate positive or negative feedback for the next cooperation. Specifically, the tacit cooperation among the three bodies in this cooperation will further promote their next cooperation, and vice versa. For the multi-body interaction of n ($n \geq 3$) individuals, without losing generality, we only consider applying control on the first component x_1, and design the following adaptive delayed feedback controller,

$$\begin{aligned} u(t) &= -k(t)\left(\sum_{j=2}^{n} x_j(t) - (n-1)x_1(t-\tau)\right), \\ \dot{k}(t) &= h\left(\sum_{j=2}^{n} x_j(t) - (n-1)x_1(t-\tau)\right), \end{aligned} \tag{2}$$

where $k(t)$ denotes the adaptive law and h is constant, and we do not control all variables of the system, but only x_1, which is an effective strategy to save resources.

Applying controller (2) to system (1), we get the following controlled system,

$$\begin{cases} \dot{x}_1(t) = -\alpha x_1(t) + f_1(x_1(t-\sigma), \cdots, x_n(t-\sigma)) \\ \qquad - k(t)\left(\sum\limits_{j=2}^{n} x_j(t) - (n-1)x_1(t-\tau)\right), \\ \dot{x}_i(t) = -\alpha x_i(t) + f_i(x_1(t-\sigma), \cdots, x_n(t-\sigma)), \\ \dot{k}(t) = h\left(\sum\limits_{j=2}^{n} x_j(t) - (n-1)x_1(t-\tau)\right), \end{cases} \tag{3}$$

where $i = 2, 3, \cdots, n$.

Theorem 1 *Original system (1) and controlled system (3) have the same equilibrium points (including the multiplicity and number) when Assumption 1 holds, independent of the adaptive variable $k(t)$ in (3).*

Proof Since Assumption 1 is true, it can be obtained from the original system (1) that

$$\begin{cases} -\alpha x_1 + f(x_1, x_2, \cdots, x_n) = 0, \\ -\alpha x_2 + f(x_1, x_2, \cdots, x_n) = 0, \\ \vdots \\ -\alpha x_n + f(x_1, x_2, \cdots, x_n) = 0, \end{cases} \tag{4}$$

and apparently $x_1 = x_2 = \cdots = x_n = x$. Hence, the number and multiplicity of the equilibrium points in system (1) are determined by the following equation

$$\alpha x = f(x, x, \cdots, x). \tag{5}$$

Similarly, for controlled system (3), we have

$$\begin{cases} -\alpha x_1 + f(x_1, x_2, \cdots, x_n) - k\left(\sum_{j=2}^{n} x_j - (n-1)x_1\right) \\ \qquad = 0, \\ -\alpha x_2 + f(x_1, x_2, \cdots, x_n) = 0, \\ \vdots \\ -\alpha x_n + f(x_1, x_2, \cdots, x_n) = 0, \\ h\left(\sum_{j=2}^{n} x_j - (n-1)x_1\right) = 0. \end{cases} \tag{6}$$

Apply the last equation of the equation set (6) to the first to get

$$\begin{cases} -\alpha x_1 + f(x_1, x_2, \cdots, x_n) = 0, \\ -\alpha x_2 + f(x_1, x_2, \cdots, x_n) = 0, \\ \vdots \\ -\alpha x_n + f(x_1, x_2, \cdots, x_n) = 0, \\ h\left(\sum_{j=2}^{n} x_j - (n-1)x_1\right) = 0, \end{cases}$$

which is the same as equation set (4) without considering the adaptive variable $k(t)$, so the equilibrium points of controlled system (3) is also given by Eq. (5). □

Remark 2 From Theorem 1, we can know that under the condition of Assumption 1, Eq. (5) determines the equilibrium point of the original system and the controlled system. For example, if Eq. (5) (such as $\alpha x = \sum_{j=1}^{n} a_j \tanh(x)$) has only zero root, then system (1) and (3) also have only zero equilibrium point. For convenience, the equilibrium points of two systems are defined as $E_1 = (x^*, x^*, \cdots, x^*)$ and $E_2 = (x^*, x^*, \cdots, x^*, k^*)$ where x^* denotes the root of the Eq. (5), and k^* is an arbitrary constant.

Remark 3 For the fully connected system, Assumption 1 is reasonable. On the one hand, each individual x_i communicates with the rest of the individuals, which makes the nonlinear feedback received by x_i ultimately tend to be consistent. On the other hand, Assumption 1 can ensure that the equilibrium point of the controlled system can be observed, which is important for the dynamic analysis of high-dimensional systems.

2.2 Global stability

In this subsection, under the Assumptions 1-3, we use the Lyapunov method to investigate the global stability of the controlled system,

$$\begin{cases} \dot{x}_1(t) = -\alpha x_1(t) + \sum_{j=1}^{n} w_{1j} g_j(x_j(t-\sigma)) \\ \qquad - k(t)\left(\sum_{j=2}^{n} x_j(t) - (n-1)x_1(t-\tau)\right), \\ \dot{x}_i(t) = -\alpha x_i(t) + \sum_{j=1}^{n} w_{ij} g_j(x_j(t-\sigma)), \\ \dot{k}(t) = h\left(\sum_{j=2}^{n} x_j(t) - (n-1)x_1(t-\tau)\right), \end{cases} \tag{7}$$

where $i = 2, 3, \cdots, n$.

Theorem 2 *The equilibrium point E_2 of controlled system (7) is globally asymptotically stable when $-2\alpha + \beta + \gamma l^2 < 0$ is satisfied, where*

$$\beta = \max_{1 \le i \le n} \left\{ \sum_{j=1}^{n} |w_{ij}| \right\}, \gamma = \max_{1 \le j \le n} \left\{ \sum_{i=1}^{n} |w_{ij}| \right\}.$$

Proof First, make the transformation $v(t) = x_1(t) + \frac{1}{2h}k^2(t)$, so it is easy to check that

$$\begin{aligned} \dot{v}(t) &= \dot{x}_1(t) + \frac{1}{h}k(t)\dot{k}(t) = -\alpha x_1 + \sum_{j=1}^{n} w_{1j} g_j(x_j(t-\sigma)) \\ &\quad - k(t)\left(\sum_{j=2}^{n} x_j(t) - (n-1)x_1(t-\tau)\right) \\ &\quad + \frac{1}{h}k(t)h\left(\sum_{j=2}^{n} x_j(t) - (n-1)x_1(t-\tau)\right) \\ &= -\alpha x_1(t) + \sum_{j=1}^{n} w_{1j} g_j(x_j(t-\sigma)). \end{aligned}$$

Equivalently, system (7) is rewritten as

$$\begin{cases} \dot{v}(t) = -\alpha x_1(t) + \sum_{j=1}^{n} w_{1j} g_j(x_j(t-\sigma)), \\ \dot{x}_2(t) = -\alpha x_2(t) + \sum_{j=1}^{n} w_{2j} g_j(x_j(t-\sigma)), \\ \qquad \vdots \\ \dot{x}_n(t) = -\alpha x_n(t) + \sum_{j=1}^{n} w_{nj} g_j(x_j(t-\sigma)). \end{cases} \tag{8}$$

Then construct a Liapunov function as

$$V(t) = \sum_{i=2}^{n} x_i^2(t) + v^2(t) + \gamma \sum_{j=1}^{n} \int_{t-\sigma}^{t} g_j^2(x_j(s))ds.$$

Calculating the derivative $\dot{V}(t)$ of $V(t)$ along the solution of (8), one has

$$\begin{aligned}\dot{V}(t) &= -2\alpha \sum_{i=2}^{n} x_i^2(t) + 2\sum_{i=2}^{n}\sum_{j=1}^{n} w_{ij} x_i(t) g_j(x_j(t-\sigma)) \\ &\quad - 2\alpha x_1(t)v(t) + 2\sum_{j=1}^{n} w_{ij} v(t) g_j(x_j(t-\sigma)) \\ &\quad + \gamma \sum_{j=1}^{n} g_j^2(x_j(t)) - \gamma \sum_{j=1}^{n} g_j^2(x_j(t-\sigma)).\end{aligned}$$

On account of $v(t) = x_1(t) + \frac{1}{2h}k^2(t)$, we can choose the appropriate constant h to meet $-\alpha x_1(t)v(t) \leq -\alpha v^2(t)$. Hence, for sufficiently large α, we have

$$\begin{aligned}\dot{V}(t) &\leq -2\alpha \sum_{i=2}^{n} x_i^2(t) + \sum_{i=2}^{n}\sum_{j=1}^{n} |w_{ij}| \left(x_i^2(t) + g_j^2(x_j(t-\sigma))\right) \\ &\quad - 2\alpha v^2(t) + \sum_{j=1}^{n} |w_{1j}| \left(v^2(t) + g_j^2(x_j(t-\sigma))\right) \\ &\quad + \gamma \sum_{j=1}^{n} g_j^2(x_j(t)) - \gamma \sum_{j=1}^{n} g_j^2(x_j(t-\sigma)) \\ &= -2\alpha \left(\sum_{i=2}^{n} x_i^2(t) + v^2(t)\right) + \beta \left(\sum_{i=2}^{n} x_i^2(t) + v^2(t)\right) \\ &\quad + \gamma \sum_{j=1}^{n} g_j^2(x_j(t-\sigma)) + \gamma l^2 \sum_{j=1}^{n} x_j^2(t) \\ &\quad - \gamma \sum_{j=1}^{n} g_j^2(x_j(t-\sigma)) \\ &\leq \left(-2\alpha + \beta + \gamma l^2\right) \left(\sum_{i=2}^{n} x_i^2(t) + v^2(t)\right).\end{aligned}$$

Now, by the standard Liapunov theorem in functional differential equation, for $-2\alpha + \beta + \gamma l^2 < 0$, the solution of (7) is globally asymptotically stable. □

2.3 Hopf bifurcation in a three-body controlled system

Now, we attempt to apply the controller to system (1) with three-body interaction to analyze its local stability and bifurcation, and the controlled system is as follows

$$\begin{cases} \dot{x}(t) = -\alpha x + f(x(t-\sigma), y(t-\sigma), z(t-\sigma)) + u(t), \\ \dot{y}(t) = -\alpha y + f(x(t-\sigma), y(t-\sigma), z(t-\sigma)), \\ \dot{z}(t) = -\alpha z + f(x(t-\sigma), y(t-\sigma), z(t-\sigma)), \end{cases} \tag{9}$$

where controller $u(t)$ meets

$$\begin{aligned} u(t) &= -k(t)(y(t) + z(t) - 2x(t-\tau)), \\ \dot{k}(t) &= h(y(t) + z(t) - 2x(t-\tau)), \end{aligned} \tag{10}$$

and Assumption 1 is satisfied.

To investigate the dynamic properties, the associated characteristic equation of linearized system (9) at the equilibrium point $E_2(x^*, x^*, x^*, k^*)$ can be obtained as follows

$$\begin{aligned}\lambda \Big\{&(\lambda+\alpha)^3 + p_{11}(\lambda+\alpha)e^{-\lambda(\sigma+\tau)} + p_{12}(\lambda+\alpha)^2 e^{-\lambda\sigma} \\ &+ \left[p_{13}(\lambda+\alpha)^2 + p_{14}(\lambda+\alpha)\right] e^{-\lambda\tau}\Big\} = 0,\end{aligned} \tag{11}$$

where $p_{11} = 2k^*(b+c)$, $p_{12} = -2k^*$, $p_{13} = -(a+b+c)$, $p_{14} = 2ak^*$, and $a = f_x(0,0,0)$, $b = f_y(0,0,0)$ and $c = f_z(0,0,0)$.

Remark 4 It is easy to see that the parameters of characteristic equation (11) contain arbitrary constant k^*, which means that Eq. (11) represents a set of characteristic equations of controlled system (9), thus providing the possibility for the multistability in phase plane. In particular, when $k^* = 0$, the characteristic equation is converted to

$$\lambda(\lambda+\alpha)^2 \left[\lambda + \alpha - (a+b+c)e^{-\lambda\sigma}\right] = 0,$$

which is not affected by feedback delay τ.

Theorem 3 *For $\sigma = 0$ and $\tau = 0$, if $\alpha < 0$ or $-\alpha + r > 0$ is satisfied, then equilibrium point $E_2(x^*, x^*, x^*, k^*)$ is unstable, where* $r = \frac{-(p_{12}+p_{13}) + \sqrt{(p_{12}+p_{13})^2 - 4(p_{11}+p_{14})}}{2}$.

Proof When $\sigma = 0$ and $\tau = 0$, characteristic equation (11) can be rewritten as

$$\begin{aligned}\lambda(\lambda+\alpha)\Big[&(\lambda+\alpha)^2 + (p_{12} \\ &+ p_{13})(\lambda+\alpha) + (p_{11}+p_{14})\Big] = 0,\end{aligned} \tag{12}$$

and its four roots are

$$\lambda_1 = 0, \lambda_2 = -\alpha,$$

$$\lambda_3 = -\alpha + \frac{-(p_{12}+p_{13}) - \sqrt{(p_{12}+p_{13})^2 - 4(p_{11}+p_{14})}}{2},$$

$$\lambda_4 = -\alpha + \frac{-(p_{12}+p_{13}) + \sqrt{(p_{12}+p_{13})^2 - 4(p_{11}+p_{14})}}{2}.$$

Emphatically, if $\alpha < 0$ or $-\alpha + r > 0$ holds, then the characteristic equation (12) has a positive root λ_2 or λ_4, that is, the equilibrium point is unstable. □

The following two cases are discussed as controlled systems with time delay.

Case I: $\sigma = 0$ and $\tau > 0$. In this case, characteristic equation (11) is equivalent to

$$\lambda(\lambda+\alpha)\Big[(\lambda+\alpha)^2 + p_{12}(\lambda+\alpha) + (p_{13}(\lambda+\alpha) + p_{11} + p_{14})\,e^{-\lambda\tau}\Big] = 0,$$

and only the transcendental equation part of the above equation is considered to investigate the existence of Hopf bifurcation of the system,

$$(\lambda+\alpha)^2 + p_{12}(\lambda+\alpha) + [p_{13}(\lambda+\alpha) + p_{11} + p_{14}]\, e^{-\lambda\tau} = 0. \tag{13}$$

Suppose that Eq. (13) has a pair of pure virtual roots defined as $\lambda'_1 = \mathrm{i}\omega$ and $\lambda'_2 = -\mathrm{i}\omega$, then we have

$$(\mathrm{i}\omega+\alpha)^2 + [p_{13}(\mathrm{i}\omega+\alpha) + p_{11} + p_{14}]\,(\cos\tau\omega - \mathrm{i}\sin\tau\omega) + p_{12}(\mathrm{i}\omega+\alpha) = 0.$$

Separating the real part and the imaginary part of the above equation yields

$$\begin{cases} p_{12}\alpha + \alpha^2 - \omega^2 + (p_{13}\alpha + p_{11} + p_{14})\cos\tau\omega \\ \qquad + p_{13}\omega\sin\tau\omega = 0, \\ p_{12}\omega + 2\alpha\omega + p_{13}\omega\cos\tau\omega \\ \qquad - (p_{13}\alpha + p_{11} + p_{14})\sin\tau\omega = 0, \end{cases}$$

and further

$$s^2 + q_1 s + q_2 = 0, \tag{14}$$

where $s = \omega^2$ and $q_1 = (p_{12}+2\alpha)^2 - 2(\alpha^2 + p_{12}\alpha) - p_{13}^2$, $q_2 = (\alpha^2 + p_{12}\alpha)^2 - (p_{13}\alpha + p_{11} + p_{14})$. The distribution of the root of Eq. (14) can be summarized as follows.

Lemma 1 *Eq. (14) has only one positive root when $q_2 < 0$, and two different positive roots when $q_2 > 0$, $q_1 < 0$, $q_1^2 - 4q_2 > 0$, otherwise there is no positive root.*

Without losing generality, suppose that Eq. (14) has two different positive roots s_1 and s_2, then there are positive frequencies $\omega_i = \sqrt{s_i}$ $(i = 1, 2)$ so that the key sequence of hopf bifurcation is

$$\tau_j^{(i)} = \frac{1}{\omega_i}\left\{\arccos\left(-\frac{AF_1 + BF_2}{A^2 + B^2}\right) + 2j\pi\right\}, \quad j = 0, 1, 2, \cdots,$$

with

$$F_1 = p_{12}\alpha + \alpha^2 - \omega^2,\ F_2 = p_{12}\omega + 2\alpha\omega,$$
$$A = (p_{13}\alpha + p_{11} + p_{14}),\ B = p_{13}\omega.$$

Define $\tau_0 = \min_{i=1,2}\left\{\tau_0^{(i)}\right\}$ and its corresponding frequency ω_0, differentiating both sides of characteristic Eq. (13) with respect to τ to verify the transversality condition, we have

$$2(\lambda+\alpha)\frac{d\lambda}{d\tau} - [p_{13}(\lambda+\alpha) + p_{11} + p_{14}]\,e^{-\lambda\tau}\left(\frac{d\lambda}{d\tau}\tau + \lambda\right) + p_{13}\frac{d\lambda}{d\tau}e^{-\lambda\tau} + p_{12}\frac{d\lambda}{d\tau} = 0,$$

clearly,

$$\left(\frac{d\lambda}{d\tau}\right)^{-1} = \frac{2(\lambda+\alpha) + p_{13}e^{-\lambda\tau} + p_{12}}{[p_{13}(\lambda+\alpha) + p_{11} + p_{14}]\,\lambda e^{-\lambda\tau}} - \frac{\tau}{\lambda},$$

and

$$\mathrm{Re}\left(\frac{d\lambda}{d\tau}\right)^{-1}_{\lambda=\mathrm{i}\omega_0,\tau=\tau_0} = \frac{CG - DH}{C^2 + D^2},$$

in which

$$C = 2\omega^2 + p_{12}\omega^2,\ D = \omega^3 + \alpha^2\omega + p_{12}\alpha\omega,$$
$$G = 2\alpha + p_{13}\cos\tau\omega + p_{12},\ D = 2\omega - p_{13}\sin\tau\omega,$$

which shows $sign\left[\mathrm{Re}\left(\frac{d\lambda}{d\sigma}\right)^{-1}_{\lambda=\mathrm{i}\omega_0,\tau=\tau_0}\right] \neq 0$ if and only if $CG - DH \neq 0$.

Theorem 4 *Suppose that $\sigma = 0$, $\tau > 0$ and $CG - DH \neq 0$ hold, then the equilibrium point of system (9) is locally asymptotically stable when $\tau \in (0, \tau_0)$, and unstable when $\tau \in (\tau_0, +\infty)$. In particular, system (9) undergoes a Hopf bifurcation when $\tau = \tau_0$.*

Case II: $\sigma > 0$ and $\tau \in (0, \tau_0)$. In this case, $\tau = \tau^*$ is a fixed delay, and σ is selected as Hopf bifurcation parameter. Considering only the transcendental equation, characteristic equation (11) becomes

$$(\lambda+\alpha)^2 + p_{11}e^{-\lambda(\sigma+\tau^*)} + p_{12}(\lambda+\alpha)e^{-\lambda\sigma} + [p_{13}(\lambda+\alpha) + p_{14}]\,e^{-\lambda\tau^*} = 0. \tag{15}$$

Similarly, assuming that $\lambda'_1 = \mathrm{i}\omega$ and $\lambda'_2 = -\mathrm{i}\omega$ are the roots of Eq. (15), one has

$$(\mathrm{i}\omega+\alpha)^2 + p_{11}\left[\cos(\sigma+\tau^*)\omega - \mathrm{i}\sin(\sigma+\tau^*)\omega\right] + p_{12}(\mathrm{i}\omega+\alpha)(\cos\sigma\omega - \mathrm{i}\sin\sigma\omega) + [p_{13}(\mathrm{i}\omega+\alpha) + p_{14}]\,(\cos\tau^*\omega - \mathrm{i}\sin\tau^*\omega) = 0,$$

and

$$\begin{cases} -\omega^2 + \alpha^2 + W_1 + M\cos\sigma\omega + N\sin\sigma\omega = 0, \\ 2\alpha\omega + W_2 + N\cos\sigma\omega - M\sin\sigma\omega = 0, \end{cases}$$

in which

$$W_1 = (p_{13}\alpha + p_{14})\cos\tau^*\omega + p_{13}\omega\sin\tau^*\omega,$$
$$W_2 = p_{13}\omega\cos\tau^*\omega - (p_{13}\alpha + p_{14})\sin\tau^*\omega,$$
$$M = p_{11}\cos\tau^*\omega + p_{12}\alpha,\ N = p_{12}\omega - p_{11}\sin\tau^*\omega.$$

Ulteriorly, we have

$$P(\omega) \triangleq \omega^4 - 2(\alpha^2 + W_1)\omega^2 + (\alpha^2 + W_1)^2 + (2\alpha\omega + W_2)^2 - N^2 - M^2 = 0. \tag{16}$$

Lemma 2 *Eq. (16) has at least one positive root ω^*, when*

$$\left|\alpha^2 + p_{13}\alpha + p_{14}\right| < |p_{11} + p_{12}\alpha|$$

is satisfied.

Proof First, $P(\omega)$ is a continuous function on interval $[0, +\infty)$, and under condition $\left|\alpha^2 + p_{13}\alpha + p_{14}\right| < |p_{11} + p_{12}\alpha|$, there is obviously

$$P(0) = (\alpha^2 + W_1)^2 + W_2^2 - N^2 - M^2 = \left[\alpha^2 + p_{13}\alpha + p_{14}\right]^2 - (p_{11} + p_{12}\alpha)^2 < 0.$$

On the other hand, $\lim\limits_{\omega\to+\infty} P(\omega) = +\infty$ is inherent. Therefore, according to the zero point theorem, there are a point ω^* and a subinterval $(0, m)$ of $[0, +\infty)$, so that $P(\omega^*)$=0 holds for $\omega^* \in (0, m)$. □

Moreover, the critical value of Hopf bifurcation point is given by

$$\sigma^{(j)} = \frac{1}{\omega^*}\left\{\arccos\left(-\frac{M(-(\omega^*)^2 + \alpha^2 + W_1) + N(2\alpha\omega^* + W_2)}{M^2 + N^2}\right) + 2j\pi\right\},$$
$$j = 0, 1, 2, \cdots.$$

and define $\sigma_0 = \sigma^{(0)}$. By differentiating both sides of characteristic equation (15) with respect to σ to verify the transversality condition, one has

$$\mathrm{Re}\left(\frac{d\lambda}{d\sigma}\right)^{-1}_{\lambda=\mathrm{i}\omega^*,\sigma=\sigma_0} = \frac{IK - JL}{I^2 + J^2},$$

where

$$\begin{aligned}
I &= p_{11}\omega^* \sin(\sigma_0 + \tau^*)\omega^* - p_{12}(\omega^*)^2 \cos\sigma_0\omega^* + p_{12}\omega^*\alpha \sin\sigma_0\omega^*,\\
J &= p_{11}\omega^* \cos(\sigma_0 + \tau^*)\omega^* + p_{12}\omega^*\alpha \cos\sigma_0\omega^* + p_{12}(\omega^*)^2 \sin\sigma_0\omega^*,\\
K &= 2\alpha + \left((\omega^*)^2 + \alpha^2\right)\tau^* + p_{12}\omega^*(\alpha\cos\sigma_0\omega^* + \omega^* \sin\sigma_0\omega^*),\\
L &= 2\omega^* + 2\omega^*\tau^*\alpha + p_{12}\tau^*(\omega^* \cos\sigma_0\omega^* - \alpha \sin\sigma_0\omega^*) - p_{12} \sin\sigma_0\omega^* - p_{13} \sin\tau^*\omega^*.
\end{aligned}$$

It is apparent that if $IK - JL \neq 0$, then the transversality condition $\mathrm{Re}\left(\frac{d\lambda}{d\sigma}\right)^{-1}_{\lambda=\mathrm{i}\omega^*,\sigma=\sigma_0} \neq 0$, which leads to Theorem 5 when $\sigma > 0$ and $\tau \in (0, \tau_0)$.

Theorem 5 *If $\left|\alpha^2 + p_{13}\alpha + p_{14}\right| < |p_{11} + p_{12}\alpha|$ and $IK - JL \neq 0$ hold true, then equilibrium E_2 is locally asymptotically stable for $\sigma \in (0, \sigma_0)$, and unstable for $\sigma \in (\sigma_0, +\infty)$. Moreover, a Hopf bifurcation occurs at the equilibrium of system (9) for $\sigma = \sigma_0$.*

3 Application in neural network models

In this section, we apply controller (2) to two specific neural network models to investigate the dynamics of the controlled systems. Previously, fully connected neural networks have been studied in some literature [26–28], but the presented phenomena are only periodic solution and asymptotically stable solution.

3.1 Ternary neural network

The expression of a controlled neural network with three neurons is as follows

$$\begin{cases}
\dot{x}_1(t) = -\alpha x_1(t) + a\tanh(x_1(t-\sigma)) + b\tanh(x_2(t-\sigma)) \\
\qquad + c\tanh(x_3(t-\sigma)) - k(t)\left(x_2(t) + x_3(t) - 2x_1(t-\tau)\right), \\
\dot{x}_2(t) = -\alpha x_2(t) + a\tanh(x_1(t-\sigma)) + b\tanh(x_2(t-\sigma)) \\
\qquad + c\tanh(x_3(t-\sigma)), \\
\dot{x}_3(t) = -\alpha x_3(t) + a\tanh(x_1(t-\sigma)) + b\tanh(x_2(t-\sigma)) \\
\qquad + c\tanh(x_3(t-\sigma)), \\
\dot{k}(t) = h\left(x_2(t) + x_3(t) - 2x_1(t-\tau)\right),
\end{cases} \tag{17}$$

where x, y, z are the states of neurons at time t, and a, b, c denotes the connection weights. Obviously, the system only has a zero equilibrium point when the adaptive variable $k(t)$ is not considered.

Fix $\alpha = 1$, $a = 0.5$, $b = 0.7$ and $c = -0.6$, $h = 0.4$ and take time-delay σ and τ as variable parameter for numerical simulation. By Theorem 4 and 5, we can know that the critical value of Hopf bifurcation is $\tau_0 = 1.81$. Figure 2 shows that with the gradual increase in feedback-delay τ, the dynamics of system (17) changes from a single asymptotically stable solution (see Fig. 2a for $\tau = 1.4 < \tau_0$) into the coexistence of asymptotically stable solution and bi-periodic solution (see Fig. 2d), where an asymptotically stable solution (blue, labeled AS) initiating from (1.4, 1.3, 1.2, 1.2) coexists with periodic solution (red, labeled

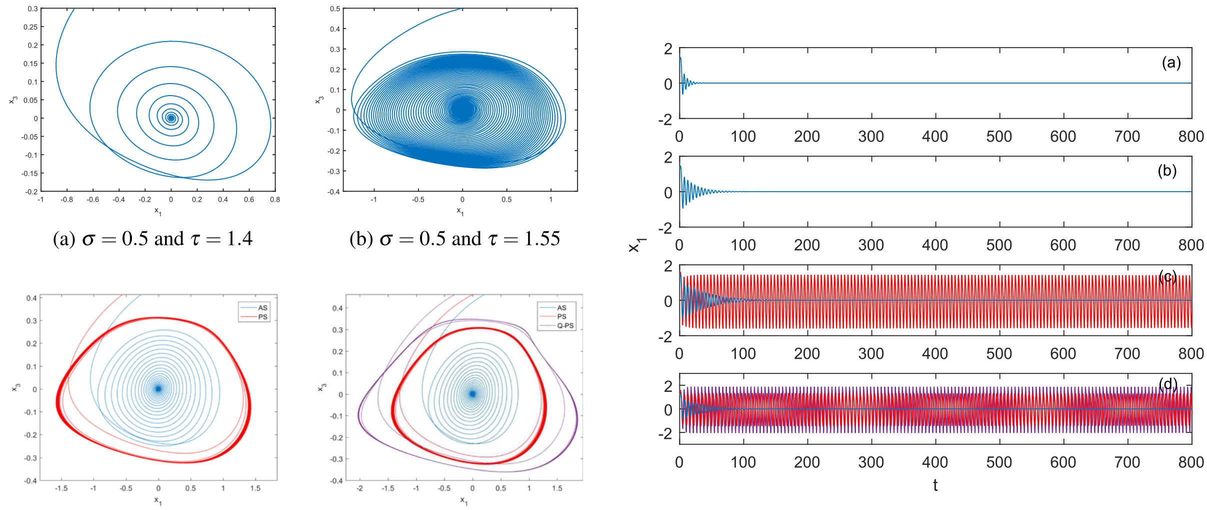

(a) $\sigma = 0.5$ and $\tau = 1.4$ (b) $\sigma = 0.5$ and $\tau = 1.55$

(c) $\sigma = 0.5$ and $\tau = 1.6$ (d) $\sigma = 0.5$ and $\tau = 1.7$ (e) time sequences

Fig. 2 Numerical results of network (17). (**a**, **b**) The trivial equilibrium point of the network is locally asymptotically stable. (**c**) An asymptotically stable solution and a periodic solution. (**d**) An asymptotically stable solution and a periodic solution, a quasi-periodic solution. (**e**) Time sequences of (**a**)–(**d**)

Fig. 3 Complex coexistence dynamic phenomenon of network (17). (**a**) An asymptotically stable solution, a periodic solution and two quasi-periodic solutions. (**b**) An asymptotically stable solution, four periodic solutions, a quasi-periodic solution and a chaotic behavior

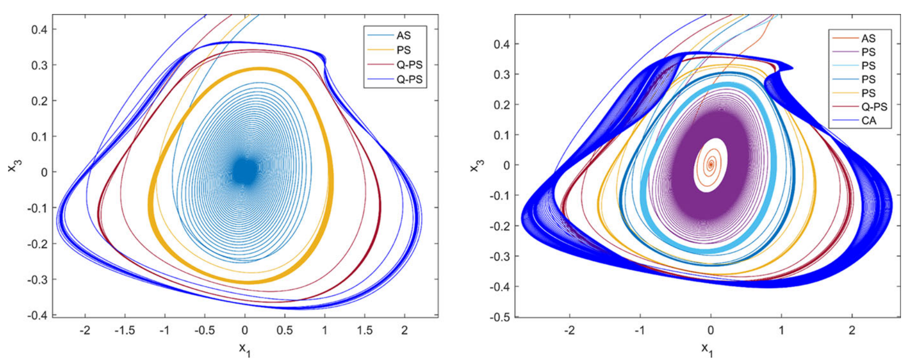

(a) $\sigma = 0.5$ and $\tau = 1.8$ (b) $\sigma = 0.5$ and $\tau = 1.9$

PS) initiating from (1.5, 1.3, 1.1, 1.2) near trivial equilibrium point in Fig. 2c, and in Fig. 2d, an asymptotically stable solution (blue, labeled AS) initiating from (1.3, 1.3, 1, 1.1) coexists with a periodic solution (red, labeled PS) initiating from (1.4, 1.3, 1.2, 1.2) and a quasi-periodic solution (purple, labeled Q-PS) initiating from (1.5, 1.3, 1.1, 1.2) near the trivial equilibrium point. Moreover, when the feedback-delay τ is further increased, the more complex coexistence phenomenon near the zero equilibrium point will appear. Specifically, an asymptotically stable solution, a quasi-periodic solution and two periodic solutions coexist in Fig. 3a, and from inside to outside, the dynamic phenomena are: asymptotically stable solution (blue, labeled AS) with initial value (1.3, 1.3, 1.1, 1), periodic solution (orange, labeled PS) with initial value (1.3, 1.3, 1, 1.1), periodic solution (dark red, labeled PS) with initial value (1.4, 1.3, 1.2, 1.2), quasi-periodic solution (dark blue, labeled Q-PS) with initial value (1.5, 1.3, 1.1, 1.2). In addition, an asymptotically stable solution, four periodic solutions, a quasi-periodic solution and a chaotic behavior coexist in Fig. 3b, and from inside to outside, the dynamic phenomena are: asymptotically stable solution (red, labeled AS) with initial value (1, 3, 1.1, 1), periodic solution (purple, labeled PS) with initial value (1.2, 1.3, 1.3, 1.1), periodic solution (blue-green, labeled PS) with initial value (1.2, 1.3, 1.4, 1.2), periodic solution (blue, labeled PS) with initial value

Fig. 4 Numerical results of network (17). (**a**) An asymptotically stable solution and two periodic solutions. (**b**) Two chaotic attractors. (**c**) Two chaotic attractors and a quasi-periodic solution, a periodic solution. (**d**) A chaotic attractor

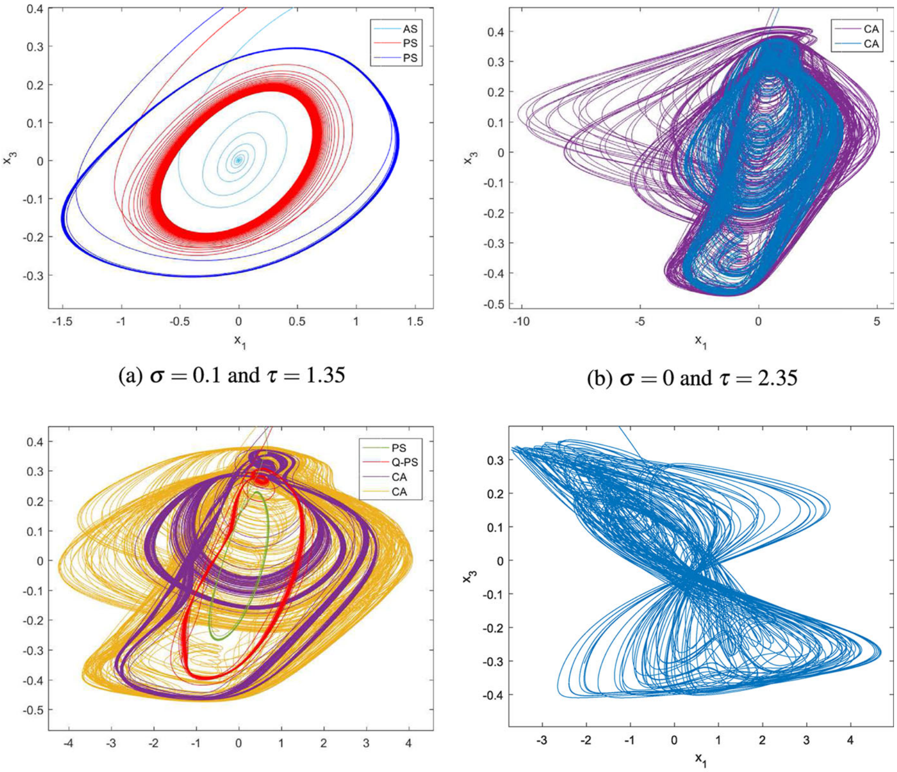

(a) $\sigma = 0.1$ and $\tau = 1.35$

(b) $\sigma = 0$ and $\tau = 2.35$

(c) $\sigma = 0.1$ and $\tau = 2.35$

(d) $\sigma = 2.7$ and $\tau = 2.9$

(1.3, 1.3, 1.1, 1), periodic solution (orange, labeled PS) with initial value (1.3, 1.3, 1, 1.1), quasi-periodic solution (dark red, labeled Q-PS) with initial value (1.4, 1.3, 1.2, 1.2), chaotic behavior (dark blue, labeled CA) with initial value (1.5, 1.3, 1.1, 1.2).

By changing the values of σ and τ, we also found some non-trivial phenomena. For example, in Fig. 4a, an asymptotically stable solution (blue, labeled AS) initiating from (1.2, 1.3, 1.4, 1.2) coexists with two periodic solutions (red, labeled PS and dark blue, labeled PS) initiating from (1.4, 1.3, 1.2, 1.2) and (1.5, 1.3, 1.1, 1.2) near the trivial equilibrium point. Figure 4b shows the coexistence of two chaotic attractors (blue, labeled CA and purple, labeled CA) initiating from (1.2, 1.3, 1.4, 1.2) and (1.3, 1.3, 1, 1.1) near the trivial equilibrium point, while Fig. 4c shows the coexistence of two chaotic attractors (orange, labeled CA and purple, labeled CA) initiating from (1.2, 1.3, 1.4, 1.2) and (1.3, 1.3, 1, 1.1), and a quasi-periodic solution (red, labeled Q-PS) initiating from (0.7, 0.9, 0.7, 0.9) and a periodic solution (dark green, labeled PS) initiating from (1, 1.3, 1.1, 1) near the trivial equilibrium point. A single chaotic attractor (blue) with initial value (1.4, 1.3, 1.2, 1.2) is shown in Fig. 4d. These phenomena illustrate that under the action of controller $u(t)$, the dynamic property of the neural network model changes from simple asymptotic stability into complex coexistence, and further show that multi-body interactive feedback can cause non-trivial dynamics of the system. Figure 5 shows the maximum Lyapunov exponent of network (17) as a function of connection weight b and delay τ, from which we can see that the maximum Lyapunov exponent of the system is greater than 0 for most parameters, indicating that chaotic attractor generally exist in the controlled system.

From the above numerical results, we can conclude that when the time-delay σ and τ are small, the controlled network (17) presents a single asymptotic stability phenomenon, while the complex coexistence of periodic and chaotic attractors will occur when σ and τ are large.

3.2 Quaternary neural network

Now, we consider a four-body interaction feedback, namely the following four-neuron fully connected net-

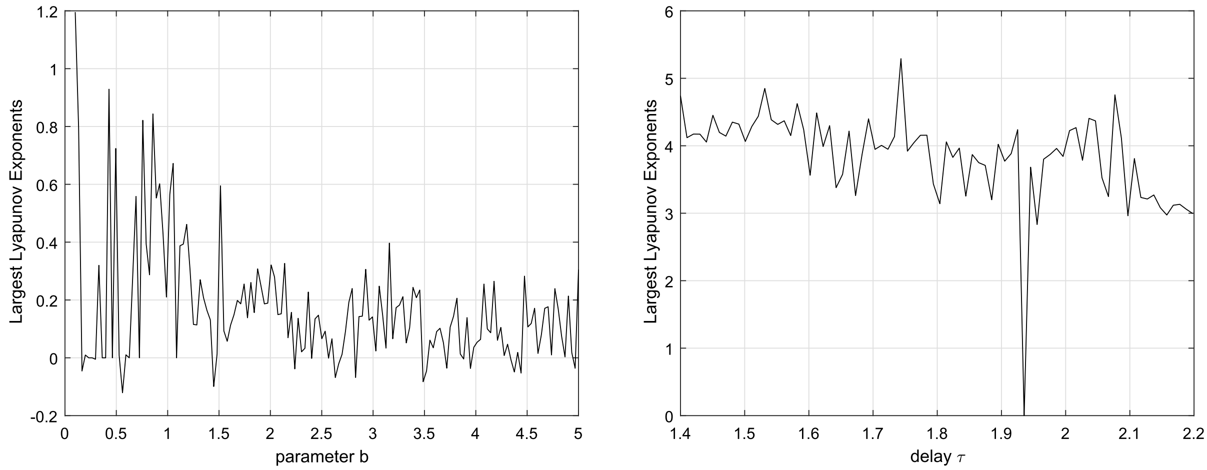

Fig. 5 The maximum Lyapunov exponent of network (17). (**a**) $\tau = 0$. (**b**) $\tau > 0$

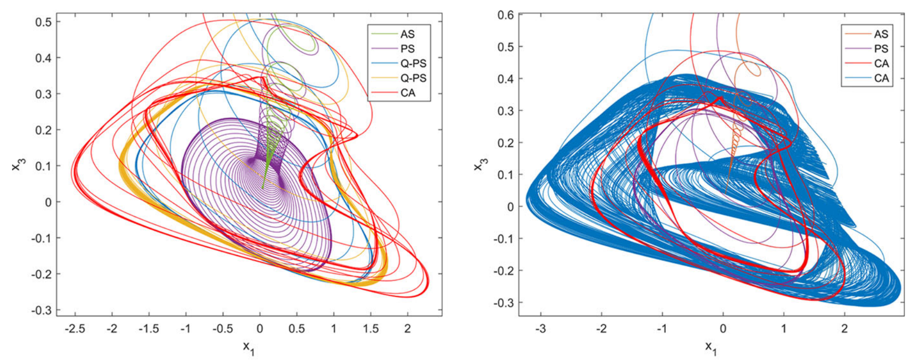

(a) $\sigma = 0.5$ and $\tau = 1.8$ (b) $\sigma = 0.5$ and $\tau = 1.9$

Fig. 6 Numerical results of network (18). (**a**) An asymptotically stable solution, a periodic solution, two quasi-periodic solutions and a chaotic behavior. (**b**) A more irregular chaotic attractor and an asymptotically stable solution, a periodic solution and a chaotic behavior

work,

$$\begin{cases} \dot{x}_1(t) = -\alpha x_1(t) + a\tanh(x_1(t-\sigma)) + b\tanh(x_2(t-\sigma)) \\ \quad + c\tanh(x_3(t-\sigma)) + d\tanh(x_4(t-\sigma)) \\ \quad - k(t)(x_2(t) + x_3(t) + x_4(t) - 3x_1(t-\tau)), \\ \dot{x}_2(t) = -\alpha x_2(t) + a\tanh(x_1(t-\sigma)) + b\tanh(x_2(t-\sigma)) \\ \quad + c\tanh(x_3(t-\sigma)) + d\tanh(x_4(t-\sigma)), \\ \dot{x}_3(t) = -\alpha x_3(t) + a\tanh(x_1(t-\sigma)) + b\tanh(x_2(t-\sigma)) \\ \quad + c\tanh(x_3(t-\sigma)) + d\tanh(x_4(t-\sigma)), \\ \dot{x}_4(t) = -\alpha x_4(t) + a\tanh(x_1(t-\sigma)) + b\tanh(x_2(t-\sigma)) \\ \quad + c\tanh(x_3(t-\sigma)) + d\tanh(x_4(t-\sigma)), \\ \dot{k}(t) = h(x_2(t) + x_3(t) + x_4(t) - 3x_1(t-\tau)), \end{cases} \tag{18}$$

where the meaning of system parameters is the same as that of network (17). Similarly, select parameter set $\alpha = 1$, $a = 0.5$, $b = 0.7$, and $c = -0.6$, $d = 0.4$, $h = 0.4$ to study the impact of time-delay on the dynamics of network (18). It is easy to see from Fig. 6 that the complex coexistence phenomena will also arise in the controlled quaternion neural network model. In Fig. 6a, there are an asymptotically stable solution, one periodic solution, two quasi-periodic solutions and one chaotic behavior coexisting near the non-trivial equilibrium point, and from inside to outside, the dynamic phenomena are: asymptotically stable solution (dark green, labeled AS) with initial value (1.2, 1.3, 1.4, 1.2, 1), periodic solution (purple, labeled PS) with initial value (1.2, 1.3, 1.3, 1.1, 1), quasi-periodic solution (blue, labeled Q-PS) with initial value (1.3, 1.3, 1, 1.1, 1), quasi-periodic solution (orange, labeled Q-PS) with initial value (1.4, 1.3, 1.2, 1.2, 1), and chaotic behavior (red, labeled CA) with initial value (1.5, 1.3, 1.1, 1.2, 1). Fig 6b shows that a more irregular chaotic attractor and an asymptotically stable solution, a periodic solution and a chaotic behavior coexist, and from inside to outside, the dynamic phenomena are: asymptotically stable solution (light red, labeled AS) with initial value (1, 1.3, 1.1, 1, 1), periodic solution (purple, labeled PS) with initial value (1.2, 1.3, 1.3, 1.1, 1), chaotic behav-

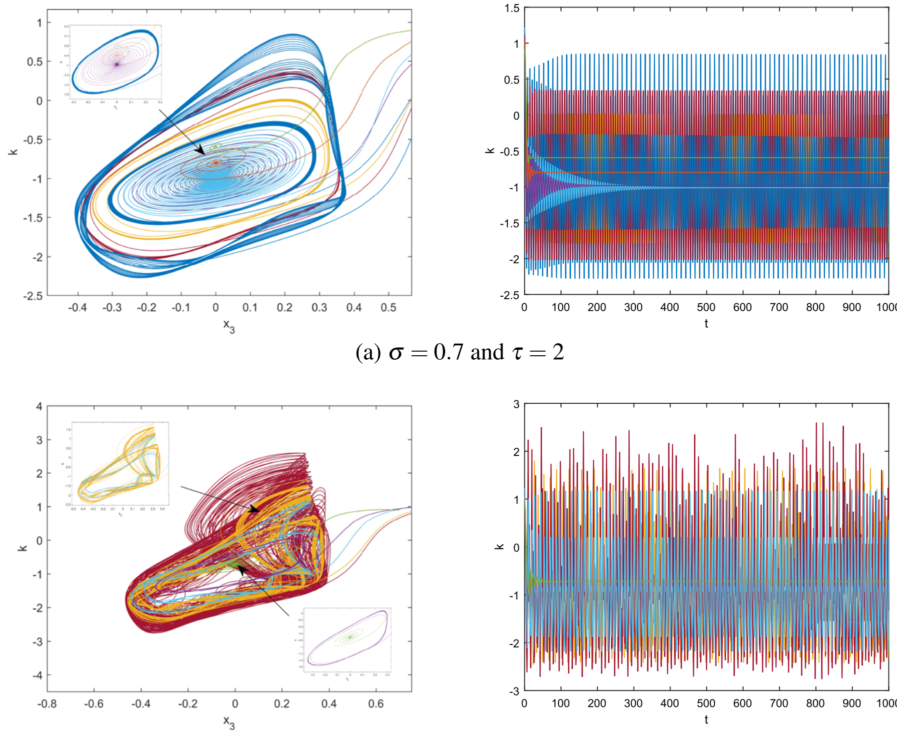

(a) $\sigma = 0.7$ and $\tau = 2$

(b) $\sigma = 0.7$ and $\tau = 2.5$

Fig. 7 Numerical results of network (17). (**a**) Complex coexistence phenomena near the different equilibrium points. (**b**) Complex coexistence phenomena near the same equilibrium point

ior (red, labeled CA) with initial value (1.3, 1.3, 1.1, 1, 1), and chaotic attractor (blue, labeled CA) with initial value (1.5, 1.3, 1.1, 1.2, 1).

In fact, complex coexistence also widely exists in higher-dimensional neural network models, and the larger the time-delay σ and τ, the more obvious these phenomena are.

Remark 5 For the numerical results presented in Figs. 2, 4 and 6, we do not consider the adaptive variable $k(t)$. In fact, various coexistence phenomena are not necessarily near the same equilibrium point, which is due to the uncertainty of k^*. For example, Fig. 7a, b show the coexistence coexistence phenomena near different and same equilibrium points of system (17) in the $x_3 - k$ plane.

4 Conclusion and discussion

This paper proposes an adaptive multi-body interactive feedback controller for fully connected system, and observes the complex coexistence phenomenon (up to seven states) in the controlled neural network model, which shows that multi-body interactive feedback can indeed improve the dynamics of system. Moreover, we have conducted theoretical analysis from the perspective of local bifurcation and global stability and grasped the theoretical mechanism of these phenomena. In the future, there are still some points worth exploring. For example,

1. How many periodic solutions and chaotic attractors can coexist at most, and the corresponding delay upper bound.
2. Whether the system dimension has an impact on the coexistence.
3. And whether there is still bright performance in real data or practical application.

These dynamic studies in fully connected system will be the focus of follow-up work.

Acknowledgements The author is grateful to all anonymous reviewers for their valuable comments, which has provided great help for the improvement of the paper.

Funding No funding was received to assist with the preparation of this manuscript.

Data availibility All data generated or analysed during this study are included in this published article (and its supplementary information files).

Declarations

Conflict of interest The authors declare that they have no conflict of interest.

Ethical approval The authors certify that this manuscript is original and has not been published and will not be submitted elsewhere for publication while being considered by Nonlinear Dynamics, and all data supporting the findings of this study are included in this manuscript.

Consent to participate This article does not contain any studies with human participants or animals performed by any of the authors.

References

1. Kuznetsov, Y.A., Kuznetsov, I.A., Kuznetsov, Y.: Elements of Applied Bifurcation Theory, vol. 112. Springer, Singapore (1998)
2. Dai, Q.: Two-parameter bifurcations analysis of a delayed high-temperature superconducting maglev model with guidance force. Chaos **32**(8), 083128 (2022)
3. Church, K.E., Liu, X.: Computation of centre manifolds and some codimension-one bifurcations for impulsive delay differential equations. J. Differ. Equ. **267**(6), 3852–3921 (2019)
4. Eskandari, Z., Alidousti, J., Ghaziani, R.K.: Codimension-one and-two bifurcations of a three-dimensional discrete game model. Int. J. Bifurcat. Chaos **31**(02), 2150023 (2021)
5. Farmer, J.D.: Chaotic attractors of an infinite-dimensional dynamical system. Phys. D **4**(3), 366–393 (1982)
6. Hunt, B.R., Kennedy, J.A., Li, T.Y., Nusse, H.E.: The Theory of Chaotic Attractors. Springer Science & Business Media, Singapore (2013)
7. Chen, C., Min, F., Zhang, Y., Bao, B.: Memristive electromagnetic induction effects on hopfield neural network. Nonlin. Dyn. **106**, 2559–2576 (2021)
8. Linsay, P.S.: Period doubling and chaotic behavior in a driven anharmonic oscillator. Phys. Rev. Lett. **47**(19), 1349 (1981)
9. Stollenwerk, N., Sommer, P.F., Kooi, B., Mateus, L., Ghaffari, P., Aguiar, M.: Hopf and torus bifurcations, torus destruction and chaos in population biology. Ecol. Complex. **30**, 91–99 (2017)
10. Ablowitz, M.J., Schober, C., Herbst, B.M.: Numerical chaos, roundoff errors, and homoclinic manifolds. Phys. Rev. Lett. **71**(17), 2683 (1993)
11. Åström, K.J., Wittenmark, B.: Adaptive Control. Courier Corporation, Massachusetts (2013)
12. Shtessel, Y., Edwards, C., Fridman, L., Levant, A., et al.: Sliding Mode Control and Observation, vol. 10. Springer, Singapore (2014)
13. Gawthrop, P.J., Wang, L.: Event-driven intermittent control. Int. J. Control **82**(12), 2235–2248 (2009)
14. Chen, G., Hill, D.J., Yu, X.: Bifurcation Control: Theory and Applications, vol. 293. Springer Science & Business Media, Singapore (2003)
15. Wang, H.O., Abed, E.H.: Bifurcation control of a chaotic system. Automatica **31**(9), 1213–1226 (1995)
16. Xu, C., Zhang, Q.: Bifurcation analysis of a tri-neuron neural network model in the frequency domain. Nonlin. Dyn. **76**, 33–46 (2014)
17. Dai, Q.: Exploration of bifurcation and stability in a class of fractional-order super-double-ring neural network with two shared neurons and multiple delays. Chaos Soliton. Fract. **168**, 113185 (2023)
18. Li, P.Z., Cai, Y.X., Wang, C.D., Liang, M.J., Zheng, Y.Q.: Higher-order brain network analysis for auditory disease. Neur. Process. Lett. **49**, 879–897 (2019)
19. Pržulj, N., Malod-Dognin, N.: Network analytics in the age of big data. Science **353**(6295), 123–124 (2016)
20. Vu, L., Morgansen, K.A.: Stability of time-delay feedback switched linear systems. IEEE Trans. Autom. Control **55**(10), 2385–2390 (2010)
21. Bleich, M.E., Socolar, J.E.: Stability of periodic orbits controlled by time-delay feedback. Phys. Lett. A **210**(1–2), 87–94 (1996)
22. Premraj, D., Suresh, K., Banerjee, T., Thamilmaran, K.: Control of bifurcation-delay of slow passage effect by delayed self-feedback. Chaos **27**(1), 013104 (2017)
23. Fan, D., Song, X., Liao, F.: Synchronization of coupled fitzhugh-nagumo neurons using self-feedback time delay. Int. J. Bifurcat. Chaos **28**(02), 1850031 (2018)
24. Shi, X., Wang, Z.: Adaptive synchronization of time delay hindmarsh-rose neuron system via self-feedback. Nonlin. Dyn. **69**, 2147–2153 (2012)
25. Lu, J., Wu, X., Han, X., Lü, J.: Adaptive feedback synchronization of a unified chaotic system. Phys. Lett. A **329**(4–5), 327–333 (2004)
26. Yan, X.P.: Hopf bifurcation and stability for a delayed tri-neuron network model. J. Comput. Appl. Math. **196**(2), 579–595 (2006)
27. Fan, D., Wei, J.: Hopf bifurcation analysis in a tri-neuron network with time delay. Nonlin. Anal. **9**(1), 9–25 (2008)
28. Mao, X., Hu, H.: Stability and bifurcation analysis of a network of four neurons with time delays. J. Comput. Nonlin. Dyn. **5**(4), 469525 (2010)